Journal of Laser Applications

Effect of laser power on conductivity and morphology of silver nanoparticle thin films prepared by a laser assisted electrospray deposition method

Cite as: J. Laser Appl. **33**, 012034 (2021); https://doi.org/10.2351/7.0000331
Submitted: 30 November 2020 . Accepted: 30 November 2020 . Published Online: 04 January 2021

Pawan Pathak, Eduardo Castillo-Orozco, Ranganathan Kumar, Aravinda Kar, and Hyoung J. Cho

COLLECTIONS

Paper published as part of the special topic on Proceedings of the International Congress of Applications of Lasers & Electro-Optics (ICALEO® 2020) ICALEO2020

Journal of Laser Applications ARTICLE scitation.org/journal/jla

Effect of laser power on conductivity and morphology of silver nanoparticle thin films prepared by a laser assisted electrospray deposition method

Cite as: J. Laser Appl. 33, 012034 (2021); doi: 10.2351/7.0000331
Submitted: 30 November 2020 · Accepted: 30 November 2020 ·
Published Online: 4 January 2021

Pawan Pathak,[1] Eduardo Castillo-Orozco,[1,2] Ranganathan Kumar,[1] Aravinda Kar,[1,3] and Hyoung J. Cho[1]

AFFILIATIONS

[1]Department of Mechanical and Aerospace Engineering, University of Central Florida, Orlando, Florida 32816
[2]Escuela Superior Politécnica del Litoral, ESPOL, Facultad en Ingeniería Mecánica y Ciencias de la Producción, Campus Gustavo Galindo, Km. 30.5 Vía Perimetral, P.O. Box 09-01-5863 Guayaquil, Ecuador
[3]CREOL, The College of Optics and Photonics, University of Central Florida, Orlando, Florida 32816

Note: Paper published as part of the special topic on Proceedings of the International Congress of Applications of Lasers & Electro-Optics 2020.

ABSTRACT

Silver nanoparticle-based electrodes were studied extensively in recent years as an electrode material for wearable and flexible electronics due to their stability and conductivity. A wet chemical deposition technique is considered as a low-cost scalable technique. The current wet chemical-based nanoparticle deposition techniques include electrospray deposition, drop casting, spin coating, and the inkjet printing process. These techniques generally require a separate postdeposition annealing step. This can be a problem for substrates with a low melting point. In addition, some of the above-mentioned methods require physical contact, which increases the probability of cross-contamination. In this research, we present a technique that combines electrospray and laser radiation to deposit and sinter nanoparticles simultaneously on a rigid or flexible substrate. In this process, the microdroplets of aqueous silver nanoparticle suspension ejected in what is known as the microdripping mode from a metallic capillary nozzle, which can be controlled by an electric potential. A conical hollow laser beam is used to vaporize the liquid and sinter the nanoparticles at desired locations on a substrate. This is a promising technique compared to the traditional methods to fabricate conductive micropatterns due to its simplified one step deposition, suppressed cross-contamination, and applicability to various surfaces. Thin-film micropatterns of silver nanoparticles were fabricated using a Nd:YAG laser with powers from 5 to 13 W. The correlation between the grain size distribution, composition, and electrical resistivity was studied using a scanning electron microscope, energy-dispersive x ray, and four-point probe analysis. The results are comparable to the conventional thermal sintering method.

Key words: electrospray, laser sintering, nanoparticles, flexible electronics

I. INTRODUCTION

Flexible and wearable electronic devices, such as radiofrequency identification tags, smart garments, medical and cosmetic devices, sensors and actuators, solar cells, and disposable electronics, have gained considerable interest[1–3] due to their low-cost, wearability, comfortability, and real-time measurement. Conductive polymers, carbon-based nanomaterials, and metallic nanomaterials have been studied as candidate materials for the flexible electrodes.[4,5] Among these materials, the silver-based nanomaterials have advantages such as water dispersibility, mechanical robustness, cost-effectiveness, high stability, and high conductivity[6–9] and can be deposited on large surface areas.[2,10] Furthermore, silver nanoparticles are known to be safer to handle compared to carbon allotropes.[5]

When combined with wet deposition techniques, these materials enable low-cost deposition on a large surface area.[2,10] The current techniques of nanoparticle-based deposition include electrospray deposition, drop casting, spin coating, and the inkjet printing process.[11,12] These techniques generally require a separate postdeposition annealing step. This can be a problem for substrates with a low melting point. Also, some of the methods mentioned above require physical contact, which increases the probability of cross-contamination and may require cleaning after each deposition step.

We have presented a novel additive manufacturing method, the nanoparticle electrospray laser deposition (NELD) process that can deposit and sinter nanoparticles simultaneously on rigid or flexible substrates. NELD is a promising technique compared to the traditional method of fabricating conductive micropatterns because of the cost-effective usage of film materials, ability to reduce contamination in the deposited film, and versatility to postdeposit electrodes after fabricating a device by using the same equipment. In this process, microdroplets of aqueous silver nanoparticle suspension are dispensed in the microdripping mode[13,14] from a capillary nozzle, and the size and number of microdroplets produced per second are controlled by applying an electric field. A conical hollow laser beam is used to vaporize the liquid and sinter the nanoparticles at desired locations on a substrate. This paper presents the effect of laser power on the electrical and morphological properties of the resulting silver films. Thermally sintered samples at the temperature equivalent to the laser power are used for comparative study.

II. EXPERIMENTAL PROCEDURE

A. Film deposition

Silver micropatterns have been deposited on silicon substrates using the NELD process (Fig. 1) and the details of the experimental procedure can be found in Refs. 13 and 14. Silver nanoparticles (metal basis 99.95%) coated with polyvinylpyrrolidone (PVP) with 30 nm average particle size, sodium dodecyl sulfate (SDS) as a surfactant, and poly-naphthalene sulfonic acid as dispersant were used to prepare the Ag nanoparticle suspension. The silver nanoparticles, surfactant, and dispersant with concentrations 20 wt. %, 16 mM, and 4 g/l, respectively, were mixed in de-ionized water, were ultrasonicated for 30 min, and the resulting colloidal suspension was used in the NELD process.

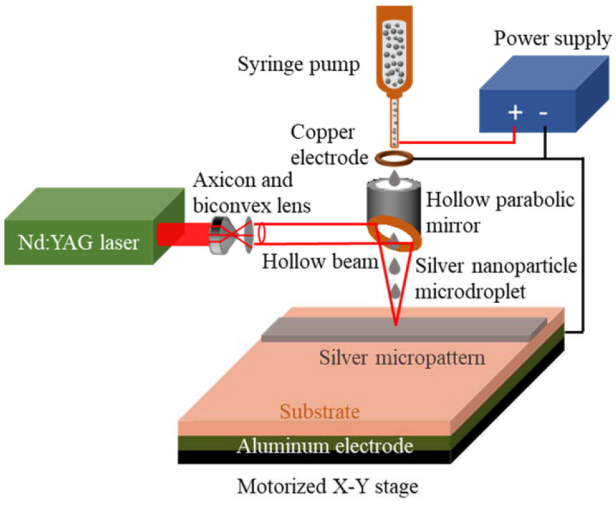

FIG. 1. Experimental setup for the nanoparticle electrospray laser deposition (NELD) process.

The Ag nanoparticle suspension was supplied to a capillary nozzle of inner diameter 0.51 mm using a syringe pump. The size of the microdroplets discharged by the nozzle and the rate of discharge are mainly controlled by two parameters, the flow rate of suspension into the nozzle and the electric field. The electric field was produced from a high electric potential (3000–3400 V) applied between the nozzle (positive electrode), an extractor, copper disk (negative electrode), and a collector electrode, aluminum plate (negative electrode) to generate monodispersed uniform microdroplets. An Nd:YAG laser of 1064 nm wavelength was used as a heat source for depositing the silver microlayers. The original Gaussian laser beam was converted into a hollow cylindrical beam using an axicon and biconvex lenses, and the beam was further reshaped into a hollow conical beam using an annular parabolic mirror to direct the apex of the laser cone onto a silicon substrate. The laser was operated at the repetition rate of 30 kHz with 170 ns pulse length, and Ag microlayers were deposited at the average laser powers of 5, 9, and 13 W. The conical laser beam was defocused to a diameter of 500 μm on the substrate surface for depositing Ag on Si without damaging the Si substrate.

The substrate was placed on a motorized X-Y stage to move the substrate continuously at the speed of 0.1 mm/s, and Ag films were deposited using microdroplets of the radius was 150 μm each. A silver line was deposited by moving the substrate with the stage while the laser heated the microdroplet, evaporated the liquid, and sintered the nanoparticles on the substrate. Silver microlayers were produced by depositing multiple lines next to each other to form a horizontal planar layer and then depositing a new planar layer on top of the previous one, thus following a technique similar to a 3D printing process. Eight silver lines were deposited on top of each other to print each section of the final microlayer.

To evaluate the performance of the NELD process, the morphology and electrical resistivity of the thin films is compared to another set of thin films prepared by drop casting silver nanoparticle suspension onto silicon wafers and sintering the resulting coating in a furnace. The time and temperature for furnace heat treatment (FHT) were selected to be similar to those in the NELD process. Both the samples were prepared under ambient conditions. The laser sintering temperature is estimated to be the temperature at the substrate surface, T(0, τ), given by[15]

$$T(0,\tau) = T_r + \left(\frac{2A\,P}{ka}\right)\left(\frac{\kappa\tau}{\pi}\right)^{1/2},$$

where T_r is the room temperature, A is the absorptivity of sliver at the wavelength (λ) of the laser and A = 0.02 at λ = 1064 nm,[16] k is the thermal conductivity (406 W m^{-1} K^{-1} for Ag), and κ is the

thermal diffusivity of the sample (1.6×10^{-4} m^2 s^{-1} for Ag).[17] P is the laser power, and a is the area of the laser beam on the substrate surface. The laser-matter interaction time for a single scan is given by $\tau = D/v \sim 2.85$ s, where D is the diameter of the laser beam and v is the speed of the substrate with respect to the laser.

The temperatures for sintering each silver line is estimated as 127, 197, and 277 °C at the laser powers 5, 9, and 13 W, respectively, for the laser-material interaction time $\tau = 2.85$ s. Since eight silver lines were deposited on top of each other to print each section of the final microlayer and assuming that localized laser heating causes minimal heat treatment in the lateral direction, the laser sintering time for the entire microlayer is considered to be $\tau_n = n\tau = 22.8$ s. Therefore, FHT samples were heated for 22.8 s at the temperatures mentioned above.

B. Characterization

The surface morphology was examined using a scanning electron microscope (SEM, Hitachi, Japan) operated at 10 kV. Elemental analysis was performed using the energy-dispersive x-ray (EDX) equipment attached to the SEM.

III. RESULTS

A. Morphological and materials characterization

Figure 2 shows the optical microscope images, SEM images, processed images, and grain size distributions for both NELD and FHT samples.

An image processing method (IMAGEJ software) was used to obtain the grain size distributions from the SEM images. The higher laser power raises the surface temperature and, therefore, enhances the interfacial fusion of nanoparticles, resulting in a larger grain size as indicated in Figs. 2(a)–2(i). This observation is in agreement with the results obtained by pulsed laser sintering processes.[18,19] The FHT samples also exhibit a similar trend as shown in Figs. 2(j)–2(r). A study by Kim *et al.* also observed a similar trend in the grain size with the processed temperature of a screen printed silver thin film.[20]

The sub-hundred micrometer lines of the silver nanoparticles were fabricated [Fig. 3(a)] on a substrate to demonstrate the applicability of the proposed NELD method to electrode fabrication on demand. Figure 3(b) shows the cross-sectional image of the sample.

Elemental analysis of the silver films was performed using EDX analysis, and Fig. 4 shows the EDX spectra for both NELD and FHT samples. The strong signals around 3.0 and 3.25 keV correspond to $L_{\alpha 1}$ and $L_{\beta 1}$ lines of the silver atom, respectively. The weak signals observed around 0.28, 0.5, and 1.0 KeV represent $K_{\alpha 1}$ lines of carbon, oxygen, and sodium atoms, respectively. The carbon, oxygen, and sodium atoms are from the PVP coating of the nanoparticles, surfactant, and dispersant. The peak intensities of C and O atoms in NELD samples decrease with an increase in the laser power [Figs. 4(a)–4(c)], indicating that the organic molecules are pyrolyzed more at higher temperatures as the power increases. A similar trend is observed for the FHT samples [Figs. 4(d)–4(f)] as the sintering temperature increases. However, the peak intensities for various impurities, such as C, O, and Na

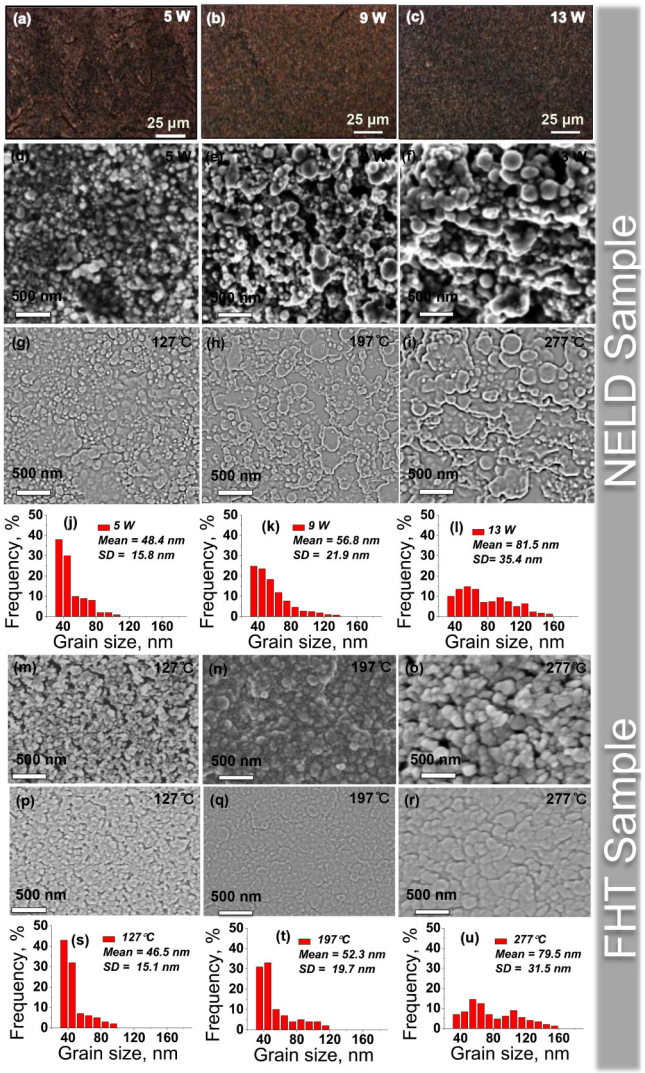

FIG. 2. NELD samples—optical microscope image [(a)–(c)], SEM images [(d)–(f)], corresponding processed images [(g)–(i)], and grain size distributions [(j)–(l)]; FHT samples—SEM images [(m)–(o)], corresponding processed images [(p)–(r)], and grain size distributions [(s)–(u)].

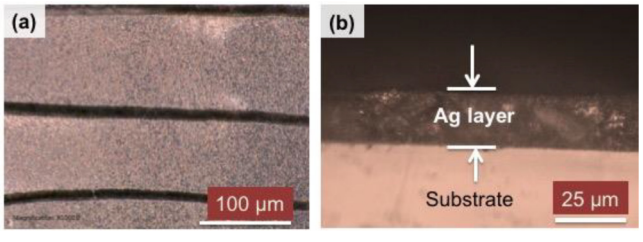

FIG. 3. Optical microscope image of silver microlines fabricated by NELD with 13 W laser power—top view (a) and cross-sectional view (b).

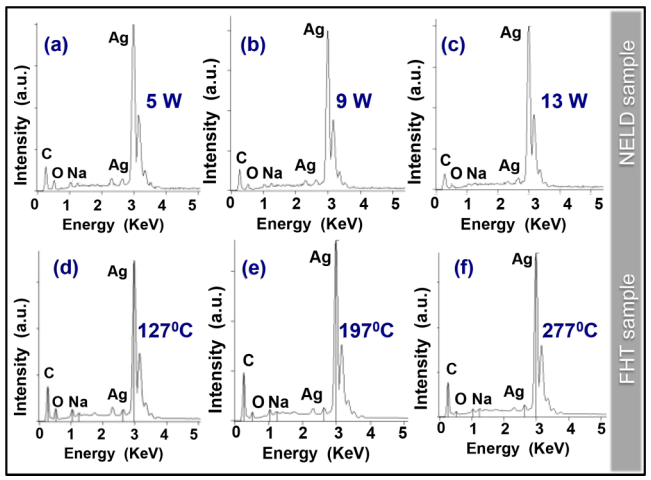

FIG. 4. EDX spectra of NELD [(a)–(c)] and FHT [(d)–(f)] samples.

atoms, in NELD samples are lower than in the FHT samples, which may be attributed to the deposition mechanisms: (i) the NELD and FHT processes involve nonequilibrium and equilibrium heating, respectively and (ii) one line at a time is deposited in the NELD process to produce the microlayer and, therefore, the impurities can diffuse out efficiently since each line has small width and thickness and is heated multiple times by the laser. In the FHT process, the microlayer is produced in a single step and, therefore, the impurities cannot diffuse out efficiently due to the large width and thickness of each microlayer.

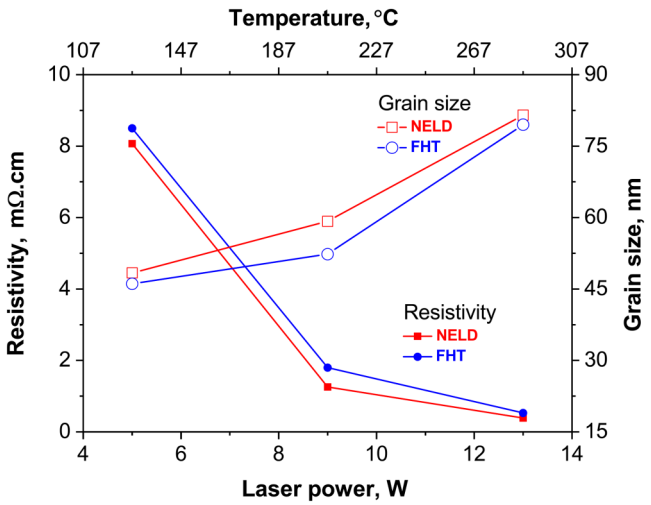

FIG. 5. Resistivity and grain size as a function of laser power. For comparative analysis, results from thermally sintered films are plotted with the equivalent laser power.

B. Electrical characterization

The electrical sheet resistances, R_s, of the samples were measured with a four-point probe, and the resistivities were calculated using the relation: $\rho = R_s t$, where t is the film thickness. The results are presented in Fig. 5 as a function of laser power (the bottom axis) and sintering temperature (the top axis) for the NELD and FHT samples, respectively. The average deviation from the mean value of the resistivity is ~15%. Figure 3(b) shows the cross-sectional image of the NELD sample prepared at 13 W indicating the film thickness to be $18 \pm 1\,\mu$m.

For both types of samples, the electrical resistivity decreases with an increase in laser power or sintering temperature since the grain size increases at higher temperatures. Similarly, the concentrations of the impurities, C, O, and Na atoms decrease at higher temperatures as shown in Fig. 3, which may also contribute to the reduction in the resistivity. The results obtained from NELD and FHT processes are within a similar range, which indicates the compatibility of NELD in place of FHT for direct writing of conductive patterns.

IV. CONCLUSIONS

The quantitative analysis of morphological and electrical characteristics of conductive films prepared by NELD was conducted. Both NELD and FHT processes exhibit a similar trend in the surface morphology, electrical conductivity, and chemical composition when the laser power increases for NELD or the temperature increases in FHT. The NELD samples, however, exhibit lower resistivity than the FHT samples since the grain size is larger, and the concentrations of the impurities are lower in the NELD samples than in the FHT samples.

ACKNOWLEDGMENTS

This work was partially supported by the National Science Foundation (NSF) under Grant No. CMMI 1563448. Special thanks to Professor Tania Roy and Ms. Adithi Krishnaprasad's assistant for resistivity measurements.

REFERENCES

[1]T. Zhang, J. Li, J. Liu, and J. Yang, "React-on-demand (RoD) fabrication of highly conductive metal–polymer hybrid structure for flexible electronics via one-step direct writing or printing," Adv. Funct. Mater. **28**, 1704671 (2018).
[2]M. Tavakoli, M. H. Malakooti, H. Paisana, Y. Ohm, D. Green Marques, P. Alhais Lopes, A. P. Piedade, A. T. Almeida, and C. Majidi, "EGaIn-assisted room-temperature sintering of silver nanoparticles for stretchable, inkjet-printed, thin-film electronics," Adv. Mater. **30**, 1801852 (2018).
[3]M. Sakai, T. Okamoto, Y. Yamazaki, J. Hayashi, S. Yamaguchi, S. Kuniyoshi, H. Yamauchi, Y. Sadamitsu, M. Hamada, and K. Kudo, "Organic thin-film transistor fabricated between flexible films by thermal lamination," Phys. Status Solidi Rapid Res. Lett. **7**, 1093–1096 (2013).
[4]R. Liu, M. Tan, X. Zhang, L. Xu, J. Chen, Y. Chen, X. Tang, and L. Wan, "Solution-processed composite electrodes composed of silver nanowires and aluminum-doped zinc oxide nanoparticles for thin-film solar cells applications," Sol. Energy Mater. Sol. Cells **174**, 584–592 (2018).
[5]B. Y. Ahn, E. B. Duoss, M. J. Motala, X. Guo, S.-I. Park, Y. Xiong, J. Yoon, R. G. Nuzzo, J. A. Rogers, and J. A. Lewis, "Omnidirectional printing of flexible, stretchable, and spanning silver microelectrodes," Science **323**, 1590–1593 (2009).

[6]I. E. Stewart, M. J. Kim, and B. J. Wiley, "Effect of morphology on the electrical resistivity of silver nanostructure films," ACS Appl. Mater. Interfaces **9**, 1870–1876 (2017).
[7]D. J. Finn, M. Lotya, and J. N. Coleman, "Inkjet printing of silver nanowire networks," ACS Appl. Mater. Interfaces **7**, 9254–9261 (2015).
[8]C. Yang, H. Gu, W. Lin, M. M. Yuen, C. P. Wong, M. Xiong, and B. Gao, "Silver nanowires: From scalable synthesis to recyclable foldable electronics," Adv. Mater. **23**, 3052–3056 (2011).
[9]Z. Liu, H. Ji, S. Wang, W. Zhao, Y. Huang, H. Feng, J. Wei, and M. Li, "Enhanced electrical and mechanical properties of a printed bimodal silver nanoparticle ink for flexible electronics," Phys. Status Solidi A **215**, 1800007 (2018).
[10]T. Kim, A. Canlier, G. H. Kim, J. Choi, M. Park, and S. M. Han, "Electrostatic spray deposition of highly transparent silver nanowire electrode on flexible substrate," ACS Appl. Mater. Interfaces **5**, 788–794 (2013).
[11]S. Bae, H. Kim, Y. Lee, X. Xu, J.-S. Park, Y. Zheng, J. Balakrishnan, T. Lei, H. Ri Kim, Y. I. Song, Y.-J. Kim, K. S. Kim, B. Özyilmaz, J.-H. Ahn, B. H. Hong, and S. Iijima, "Roll-to-roll production of 30-inch graphene films for transparent electrodes," Nat. Nanotechnol. **5**, 574–578 (2010).
[12]D. Kong, L. T. Le, Y. Li, J. L. Zunino, and W. Lee, "Temperature-dependent electrical properties of graphene inkjet-printed on flexible materials," Langmuir **28**, 13467–13472 (2012).
[13]E. Castillo-Orozco, R. Kumar, and A. Kar, "Laser-induced subwavelength structures by microdroplet superlens," Opt. Express **27**, 8130–8142 (2019).
[14]E. Castillo-Orozco, R. Kumar, and A. Kar, "Laser electrospray printing of nanoparticles on flexible and rigid substrates," J. Laser Appl. **31**, 022015 (2019).
[15]A. M. Prokhorov, *Laser Heating of Metals* (CRC Press, Boca Raton, FL, 2018).
[16]J. Springer, A. Poruba, L. Müllerova, M. Vanecek, O. Kluth, and B. Rech, "Absorption loss at nanorough silver back reflector of thin-film silicon solar cells," J. Appl. Phys. **95**, 1427–1429 (2004).
[17]W. Parker, R. Jenkins, C. Butler, and G. Abbott, "Flash method of determining thermal diffusivity, heat capacity, and thermal conductivity," J. Appl. Phys. **32**, 1679–1684 (1961).
[18]P. Fischer, V. Romano, H. P. Weber, and S. Kolossov, "Pulsed laser sintering of metallic powders," Thin Solid Films **453–454**, 139–144 (2004).
[19]T. Park and D. Kim, "Excimer laser sintering of indium tin oxide nanoparticles for fabricating thin films of variable thickness on flexible substrates," Thin Solid Films, **578**, 76–82 (2015).
[20]K.-S. Kim, W.-R. Myung, and S.-B. Jung, "Effects of sintering conditions on microstructure and characteristics of screen-printed Ag thin film," Electron. Mater. Lett. **8**, 309–314 (2012).